2015

Comparative Metal Oxide Nanoparticle Toxicity Using Embryonic Zebrafish

Leah C. Wehmas
Oregon State University

Catherine Anders
Boise State University

Jordan Chess
Boise State University

Alex Punnoose
Boise State University

Cliff B. Pereira
Oregon State University

See next page for additional authors

Publication Information

Wehmas, Leah C.; Anders, Catherine; Chess, Jordan; Punnoose, Alex; Pereira, Cliff B.; Greenwood, Juliet A.; and Tanguay. Robert L. (2015). "Comparative Metal Oxide Nanoparticle Toxicity Using Embryonic Zebrafish". *Toxicology Reports, 2*, 702-715. http://dx.doi.org/10.1016/j.toxrep.2015.03.015

Toxicology Reports 2 (2015) 702–715

Contents lists available at ScienceDirect

Toxicology Reports

journal homepage: www.elsevier.com/locate/toxrep

Comparative metal oxide nanoparticle toxicity using embryonic zebrafish

Leah C. Wehmas[a], Catherine Anders[b], Jordan Chess[b], Alex Punnoose[b], Cliff B. Pereira[c], Juliet A. Greenwood[d], Robert L. Tanguay[a,*]

[a] Department of Environmental and Molecular Toxicology, Environmental Health Sciences Center, Oregon State University, 1007 Agriculture & Life Sciences Building, Corvallis, OR 97331, USA
[b] Department of Physics and the Interdisciplinary Graduate Program in Biomolecular Sciences, Boise State University, 1910 University Drive, Boise, ID 83725, USA
[c] Department of Statistics, Oregon State University, Corvallis, OR 97331, USA
[d] Department of Biochemistry and Biophysics, Environmental Health Sciences Center, Oregon State University, 2011 Agricultural & Life Sciences Building, Corvallis, OR 97331, USA

ARTICLE INFO

Article history:
Received 10 February 2015
Received in revised form 31 March 2015
Accepted 31 March 2015
Available online 2 May 2015

Keywords:
Zinc oxide
Titanium dioxide
Cerium dioxide
Tin dioxide
Nanoparticles
Zebrafish
Dissolution
ICP OES

ABSTRACT

Engineered metal oxide nanoparticles (MO NPs) are finding increasing utility in the medical field as anticancer agents. Before validation of *in vivo* anticancer efficacy can occur, a better understanding of whole-animal toxicity is required. We compared the toxicity of seven widely used semiconductor MO NPs made from zinc oxide (ZnO), titanium dioxide, cerium dioxide and tin dioxide prepared in pure water and in synthetic seawater using a five-day embryonic zebrafish assay. We hypothesized that the toxicity of these engineered MO NPs would depend on physicochemical properties. Significant agglomeration of MO NPs in aqueous solutions is common making it challenging to associate NP characteristics such as size and charge with toxicity. However, data from our agglomerated MO NPs suggests that the elemental composition and dissolution potential are major drivers of toxicity. Only ZnO caused significant adverse effects of all MO particles tested, and only when prepared in pure water (point estimate median lethal concentration = 3.5–9.1 mg/L). This toxicity was life stage dependent. The 24 h toxicity increased greatly (~22.7 fold) when zebrafish exposures started at the larval life stage compared to the 24 h toxicity following embryonic exposure. Investigation into whether dissolution could account for ZnO toxicity revealed high levels of zinc ion (40–89% of total sample) were generated. Exposure to zinc ion equivalents revealed dissolved Zn^{2+} may be a major contributor to ZnO toxicity.

1. Introduction

Engineering materials at the nanoscale results in unique characteristics valuable for applications in electronics, personal care products, environmental remediation and medicine [1,2]. The semiconducting properties of metal oxide nanoparticles (MO NPs) such as zinc oxide (ZnO) and titanium dioxide (TiO_2) make them particularly popular for use in commercially available sunscreens and cosmetics to block ultraviolet radiation when they are <50 nm in size [3]. Engineered MO NPs are finding

* Corresponding author. Tel.: +1 541 737 6514; fax: +1 541 737 6074.
E-mail addresses: wehmasl@onid.orst.edu (L.C. Wehmas), catherineanders@u.boisestate.edu (C. Anders), jchess@uoregon.edu (J. Chess), apunnoose@boisestate.edu (A. Punnoose), pereira@science.oregonstate.edu (C.B. Pereira), julie.greenwood@oregonstate.edu (J.A. Greenwood), robert.tanguay@oregonstate.edu (R.L. Tanguay).

http://dx.doi.org/10.1016/j.toxrep.2015.03.015

increasing utility in the medical field ranging from use as antimicrobial agents [3–6] to diagnostic imaging [7–13] and potential cancer treatment [5,9,14–16]. While scaling down the size of materials to the nanometer realm imparts useful traits, they are then within a size range to interact with biomolecules, such as proteins and nucleic acids, or organelles such as mitochondria, causing damage that could interfere with biological functions [1,2].

To date, most anti-cancer applications with engineered MO NPs have been demonstrated using cell lines [9,10,15,16]. Specifically, *in vitro* studies indicate ZnO nanomaterials generate reactive oxygen species, perturb calcium homeostasis within the mitochondria, disrupt cellular membranes, induce apoptosis and generate an inflammatory response [14,15,17,18]. TiO_2 nanomaterials, in the absence of photoactivation, require high parts per million exposure concentrations to affect gene transcription, cause DNA and chromosomal damage, and stimulate inflammation [19–21]. Upon photoactivation, TiO_2 nanomaterials generate more reactive oxygen species resulting in greater cytotoxicity to mammalian cells and bacteria [3,4]. Conversely, some cerium dioxide (CeO_2) nanomaterials scavenge reactive oxygen species enhancing cell survival in the presence of an oxidant [18,22], but these results are controversial as others have found the opposite effect [23,24]. Unfortunately, differences in experimental design and exposure concentrations can make cross study comparisons difficult, and evaluating the toxicity of these materials under culture conditions with a single or even a few cell types cannot adequately simulate a living dynamic organism, which can metabolize, sequester and excrete compounds. Before *in vivo* efficacy of these MO NPs as medical agents can occur, a better understanding of whole-animal nanomaterial toxicity is required. This could enable the engineering of safer nanomaterials for therapeutic applications. Despite a multitude of data on NP toxicity, data gaps still exist and the limited sample availability, common with nanomaterials under development, make *in vivo* nanotoxicology assessment particularly challenging using traditional mammalian models.

The embryonic zebrafish model has emerged as an inexpensive and efficient alternative for *in vivo* nanotoxicity screening [25,26]. This is, in part, due to the high degree of genetic conservation, anatomical and physiological similarity between zebrafish and humans particularly throughout development. Additionally, the small size, rapid growth and transparency of zebrafish embryos makes them conducive for moderate to high-throughput screening methods. Toxicity assays can be conducted in 96-well plates in which morbidity and mortality are visually assessed over a short duration. Multiple routes of nanoparticle exposure including epithelial absorption (primary), ingestion, and respiration (gill uptake) can be assessed along with identification of potential windows of developmental susceptibility to NPs. The small quantity of test material required to investigate *in vivo* toxicity in zebrafish is particularly advantageous.

Our laboratory assesses nanotoxicity using a well-defined five-day embryonic zebrafish assay [26–29]. Research by others assessing MO NP toxicity with the zebrafish model has primarily focused on characterizing ecotoxicological health risks [30–39]. These assays typically employ zebrafish embryos with intact chorions, an acellular envelope surrounding the embryo, which can obstruct NP uptake in a size dependent manner and potentially confound interpretation of concentration response results [30,39]. Furthermore, NPs are frequently coated with various natural organic matter to mimic aqueous environmental conditions, which will alter bioavailability [40–43]. Because our laboratory is interested in these NPs for medical applications, we enzymatically removed the chorion to mitigate barriers of NP absorption, and we do not coat the MO NPs with natural organic matter. Zebrafish exhibit a high degree of tolerance to varying water chemistry parameters such as salinity and pH allowing us to carefully adjust exposure conditions, such as reducing medium salt content to diminish agglomeration and enhance particle absorption [44,45].

The objective of these studies was to assess and compare the *in vivo* toxicity of seven semiconductor MO NPs made from zinc oxide (ZnO), titanium dioxide (TiO_2), cerium dioxide (CeO_2) and tin dioxide (SnO_2). In this article, we report the first *in vivo* toxicity assessment of these novel MO NPs compared to bulk controls using the embryonic zebrafish assay under two medium conditions of differing ionic strengths. While these MO NPs possess similar primary mean diameters and spherical shapes, they differ in physicochemical properties such as band gap, hydrodynamic size, charge, chemical composition and ionic state of metal ions, and reactive oxygen species generation. We hypothesized that differences in MO NP toxicity will depend on these physicochemical properties. In this study we investigated how hydrodynamic size and charge of uncoated, non-functionalized MO NPs in a waterborne suspension affected zebrafish toxicity. Most MO NPs caused little to no toxicity in our assay under either medium condition except ZnO. Similar to other aqueous systems, MO NP agglomeration complicates toxicological studies making it challenging to study primary particle characteristics, as these particles are not well dispersed, and ions present in the suspension medium can further enhance agglomeration and impede dispersal. However, it is important to note that agglomeration is an important parameter in particle hazard assessment. Despite agglomeration of all our MO NPs, particularly in the high ionic strength embryo medium, we successfully compared how size and charge were associated with the toxicity of three MO NPs: TiO_2 (TC009), CeO_2 (QK055) and ZnO, as they created stable suspension in low ionic strength water. While all three MO NPs possessed similar hydrodynamic sizes and similar, high positive charges under our assay conditions, only ZnO was significantly toxic to embryonic zebrafish. This data suggests that for MO NPs suspended in water, elemental composition or dissolution are principally important for producing toxicity in zebrafish.

2. Materials and methods

2.1. Nanoparticle synthesis

All MO NPs were produced through in-house synthesis. Bulk samples were purchased from commercially available

sources. All chemicals used in our synthesis were reagent grade. They were used without further modification unless otherwise indicated. Synthesis details of each nanomaterial system are given below.

ZnO NPs: ZnO NPs were synthesized using forced hydrolysis. Briefly 1.0 g of zinc acetate dehydrate ($Zn(CH_3COO)_2{\cdot}2H_2O$) was heated in 100 mL of diethylene glycol containing 0.5 mL of nanopure water at 160 °C for 90 min. The nanoparticles were then rinsed three times with ethanol and were separated using centrifugation for 20 min at 20,000 rpm after each rinse.

CeO_2 NPs: CeO_2 NPs were also prepared by a forced-hydrolysis process using cerium chloride as precursor. The cerium precursor was dissolved along with lithium hydroxide in ethanol, heated to 70 °C in a silicon oil bath, and held while stirring for 90 min. After heating, the solution was mixed with N-heptane to facilitate crystal growth, and allowed to rest for 20–24 h. The precipitate was centrifuged and washed in ethanol to remove any remaining precursor, and washed twice in nanopure water to remove any residual hydroxide and ethanol. The final product was dried in an oven for 24 h at 50 °C before being ground to a fine powder using an agate mortar and pestle.

SnO_2 NPs: SnO_2 NPs designated as UG022 were prepared using Tin (IV) chloride pentahydrate ($SnCl_4{\cdot}5H_2O$) and urea. The syntheses were carried out at 90 °C in nanopure water for 90 min. The SnO_2 NPs designated UG023 were prepared using Tin (IV) acetate ($Sn(C_2H_4OH)_4$) precursor. This synthesis was carried out in benzyl alcohol at 100 °C for 90 min. Samples were extracted from solution by centrifugation at 21,000 rpm before drying in an oven at 50 °C.

TiO_2 NPs: TiO_2 NPs were prepared by combining titanium isopropoxide and benzyl alcohol in a glove box maintained with nitrogen atmosphere at atmospheric pressure. Samples were stirred for 5 min prior to the addition of 0.5 mL nanopure water along with heating to 150 °C. Temperature was maintained for 24 h. Cooled NPs were centrifuged and washed using ethanol and nanopure water followed by drying in an oven for 12 h.

All the as-purchased bulk MO samples from multiple commercial sources had a small fraction of material present in them as <10 nm crystallites. The commercially acquired bulk MO samples were annealed in air at 800 °C for 3 h to sinter any nanocrystals present before using them as bulk controls.

2.2. Nanoparticle characterization

All nanoparticle samples were thoroughly characterized using x-ray diffraction (XRD), X-ray photoelectron spectroscopy (XPS), inductively coupled plasma-mass spectrometry (ICP-MS), transmission electron microscopy (TEM), Zeta potential (charge) and hydrodynamic size measurements. Room temperature XRD spectra were collected with a Philips X'Pert X-ray diffractometer using a Cu K_α source ($\lambda = 1.5418$ Å) in Bragg–Brentano geometry. Briefly, loose powder samples were leveled in the sample holder to ensure a smooth surface and mounted on a fixed horizontal sample plane. Rietveld refinement was utilized to obtain lattice parameters and crystal size using Materials Analysis Using Diffraction (MAUD) software after correction for instrumental broadening [46]. High-resolution TEM analysis was carried out on a JEOL JEM-2100HR microscope with a specified point-to-point resolution of 0.23 nm and an operating voltage of the microscope was 200 kV. Image processing was carried out using the Digital Micrograph software from Gatan (Pleasant, CA, USA).

The hydrodynamic size distribution and charge of each MO NP was measured using dynamic light scattering (DLS) with a Malvern Zetasizer Nano ZS instrument. The Malvern Zetasizer Nano ZS measures particles with diameters within 0.3 nm to 10 μm utilizing Non-Invasive Back Scatter technology and the Stokes-Einstein relationship to obtain particle size distributions based on the diffusion of particles traveling by Brownian motion. Charge is measured using Laser Doppler Micro-electrophoresis, which involves applying an electric field to particles in suspension causing them to move at a velocity, which is used to calculate electrophoretic mobility. The Helmholtz–Smoluchowski equation is employed to convert electrophoretic mobility to charge. We quantified size and charge using 50 mg MO NP per L embryo medium at 0.5% dimethyl sulfoxide (DMSO, JT Baker, Center Valley, PA, USA), pH 7 and using 50 mg MO NP per L purified, deionized water (ultrapure water, Invitrogen, Carlsbad, CA, USA) at 0.5% DMSO (the highest exposure concentrations tested in the embryonic zebrafish bioassay). Each sample was prepared using the same preparation methods as the zebrafish embryo larval exposure assay, and the samples were measured four times within 1–2 h of preparation.

2.3. Inductively coupled plasma optical emission spectrometry of zinc dissolution

Measurements of dissolved zinc present in ZnO NP suspensions were quantified by Inductively Coupled Plasma Optical Emission Spectrometry (ICP-OES) using a Teledyne Leeman instrument Prodigy (Hudson, NH, USA) and a protocol modified from Poynton et al. [47]. ZnO NP suspensions were diluted in ultrapure water to two exposure concentrations, 0.625 and 10 mg/L. ZnO bulk suspensions were diluted in ultrapure water to 10 mg/L as well. At 0, 6, 24 and 120 h post sample preparation, suspensions were filtered through a 10 kD molecular weight cutoff Macrosep centrifuge filtration unit (PALL Life Sciences, Ann Arbor, MI, USA) which will retain all particles with a diameter above ~2 nm, thereby collecting what we defined as the soluble zinc in the filtrate. Unfiltered ZnO NP and bulk suspensions were also collected to quantify total zinc concentrations to determine the percentage of dissolved zinc present in ZnO NP suspensions. Both soluble and total zinc solutions were concentrated and dissolved in 35% nitric acid overnight. Digested samples were then reconstituted to 1X and a final acid concentration of 7% in millipore water treated with chelex 100 prior to ICP-OES analysis. Analyzed samples were compared to known zinc standards (ULTRA Scientific, N. Kingstown, RI, USA). A known quantity of zinc (5 mg/L) was also run through our method to determine zinc recovery (101.5%).

2.4. Zebrafish husbandry

Adult 5D Tropical zebrafish were housed at the Sinnhuber Aquatic Research Laboratory in accordance with Institutional Animal Care and Use Committee protocols at Oregon State University. Spawning fish were maintained at 10 fish/L in 100 L tanks recirculated with reverse osmosis water reconstituted with sea salts (Instant Ocean, United Pet Group, Inc., Blacksburg, VA, USA) under a 14 h light:10 h dark photoperiod at 28 ± 1 °C. Spawning occurred in the morning, and eggs were collected by funnel and staged as documented in Kimmel et al. [48].

2.5. Zebrafish bioassays

2.5.1. Five-day embryonic zebrafish bioassay

A volume of 0.1 mL of the five-fold nanoparticle and bulk control exposure concentrations, each prepared in ultrapure water and embryo medium, was transferred to a sterile polystyrene 96-well tissue culture, flat bottom plate (Falcon, Manassas, VA). At 4 h post fertilization (hpf), the acellular chorion of the zebrafish eggs was enzymatically digested using pronase and an automated protocol described by Mandrell et al. [49]. One dechorionated embryo was transferred by glass pipet to each well of the plates for a minimum of $N = 32$ per exposure concentration of nanoparticle and bulk control in water and embryo medium. Embryos damaged during loading were excluded from the experiment. The embryos were maintained in the exposure solutions at 28 ± 1 °C for 120 h. The plates were wrapped in aluminum foil to prevent potential confounding toxicity from particle exposure to ambient light. At 24 and 120 hpf, the zebrafish were visually inspected by stereomicroscope for mortality and a suite of morphological abnormalities, which will be referred to as toxicological endpoints (see Table 2 for descriptions). Data was recorded using a binary system in which the presence of an endpoint received a score of 1 while the absence of an endpoint received a score of 0. A detailed description of this assay may be found in Truong et al., 2011 [29]. Typically, we examine 22 specific endpoints, however, exposures in low ionic strength ultrapure water, at times, resulted in variable and sometimes elevated background prevalence of malformations, which was date dependent especially for two endpoints equally across all exposure concentrations including controls. The endpoints were excluded from the results. This did not confound our toxicity assessments or statistical analyses as we always compared exposure groups to the respective controls based on the date of an experiment.

2.5.2. 96 h post fertilization larval zebrafish bioassay

A dilution series of ZnO NP, ZnO bulk or zinc ion equivalent, each prepared in ultrapure water, was transferred to a sterile polystyrene 96-well tissue culture, flat bottom plate at 0.1 mL per well. Zebrafish at 96 hpf were rinsed in water prior to loading into each plate at one fish per well with a minimum of $N = 24$ per exposure concentration. Plates were wrapped in foil to exclude light and maintained at 28 ± 1 °C. Plates were inspected for malformations and mortality at 1, 2, 6 and 24 h post exposure. Due to high lethality, we focused on mortality as the most relevant endpoint. Data was recorded as described in 2.5.1.

2.6. Nanoparticle exposures

On the day of an exposure, an aliquot of nanoparticle and bulk material control were suspended in 100% DMSO at a concentration of 10 mg/mL and water bath sonicated (Ultrasonik NDI, NEY, Inc., Bloomfield, CT, USA) for 20 min at room temperature. Immediately following sonication, the nanoparticle and bulk stock solutions were diluted to the desired exposure concentrations. For the five-day embryonic zebrafish assay, nanoparticle and bulk were diluted to 50, 10, 2, 0.4 and 0.08 mg/L in ultrapure water and diluted to 50, 10, 2, 0.4 and 0.08 mg/L in buffered, pH 7–7.2, embryo medium. Embryo medium is a defined synthetic sea solution consisting of 15 mM NaCl, 0.5 mM KCl, 1 mM $CaCl_2{:}2H_2O$, 0.15 mM KH_2PO_4, 0.05 mM Na_2HPO_4 and 1 mM $MgSO_4{:}7H_2O$ commonly used to rear zebrafish embryos and conduct embryo-larval toxicity assays. The vehicle controls consisted of 0.5% DMSO in ultrapure water and 0.5% DMSO in embryo medium. To test the toxicity of zinc ion present in ZnO NP solutions, we used the ICP-OES results from 120 h in 10 mg/L ZnO NP to calculate equivalent concentrations using $ZnSO_4{\cdot}7H_2O$, which was diluted in ultrapure water to 98.9, 19.8, 4.0, 0.8 and 0.16 mg/L with 0.5% DMSO. For the 96 hpf zebrafish bioassay, ZnO NP and ZnO bulk were suspended and sonicated as described above. ZnO NP, ZnO bulk were diluted in ultrapure water to 20, 10, 5, 2.5, 1.25, 0.625 and 0.3125 mg/L in ultrapure water with DMSO maintained at 0.5%. We used the amount of zinc ion measured by ICP-OES in the 0.625 mg/L ZnO NP sample after 24 h to calculate equivalent concentrations using $ZnSO_4{\cdot}7H_2O$ for the 96 hpf exposures. This resulted in $ZnSO_4{\cdot}7H_2O$ exposures of 42.7, 21.35, 10.68, 5.34, 2.67, 1.33 and 0.67 mg/L with DMSO maintained at 0.5%. The dissolved zinc present in 0.625 mg/L ZnO NP was selected to calculate the amount of $ZnSO_4{\cdot}7H_2O$ to use in the 96 hpf exposure because we previously found 0.625 mg/L of ZnO NP resulted in the lowest observable lethality after 24 h.

2.7. Scanning electron microscopy

Larval zebrafish at 96 hpf, were exposed to 0.5% DMSO, 0.625 and 10 mg/L ZnO NP and 10 mg/L ZnO bulk in water for ~1–2 h prior to fixation in electron microscopy fixative. Samples were prepared by placing 10, 96 hpf larvae in 1 mL of fixative consisting of 1% paraformaldehyde in 2.5% glutaraldehyde and 0.1 M sodium cacodylate buffer overnight at room temperature. Samples were rinsed twice in 0.1 M cacodylate buffer for 15 min each prior to dehydration in 30–100% acetone or ethanol for 10–15 min each. Samples then underwent critical point drying and were sputter coated with gold–palladium alloy before imaging. Images were acquired at 500× using an FEI Quanta 600 FEG scanning electron microscope.

2.8. Statistics

Within each MO, medium and nanoparticle *vs.* bulk combination, logistic regression was used to test for any

differences in proportion mortality or proportion affected across the six concentrations used in each experiment (5 d.f. test). Because of the low incidences at many concentrations for many of the combinations, exact logistic regression was employed in SAS (Cary, NC, USA) using PROC LOGISTIC. When there was evidence of concentration effects ($p < 0.0001$ for ZnO NP and zinc ion in water), median lethal concentration estimates (LC50) and median effect concentration (mortality combined with malformed) estimates (EC50) were determined by first dropping the lowest doses until there was no lack of fit to a logit linear in log concentration model and then using that model to estimate the quantities of interest (LOGIT and INVERSECL options in SAS PROC PROBIT). Fisher's Exact analysis was performed for each ZnO NP and zinc ion in water separated by experimental date ($p < 0.05$ considered significant). Within each response and experiment date, concentration above vehicle control was compared to background. Only for 10 and 50 mg/L was the prevalence significantly higher for both ZnO NP and zinc ion in water for all experiments studied.

3. Results and discussion

3.1. Metal oxide nanoparticles with similar primary particle size differ greatly in hydrodynamic size and charge

We characterized MO NP purity through XRD, XPS and ICP-MS. The primary particle size (crystallite size) of MO NP was obtained by both TEM while hydrodynamic size and charge were determined using DLS electrophoresis measurements, respectively. Detailed analyses of MO NPs using XPS confirmed that there were no unexpected elements in the samples and ICP-MS further revealed that concentrations of common impurities such as the tested Fe, Mn, Co, Ni, Cr and V ions were below 1 ng/L. TEM analyses demonstrated that all MO NPs exhibited a spherical shape (Fig. A1), and the average primary particle size of each material type was within the 2.8–11.6 nm range in diameter (Table 1). DLS data acquired for the highest exposure concentration (50 mg/L at 0.5% DMSO) indicated that none of our MO NPs stayed well suspended in embryo medium (Fig. 1, Table 1) likely due to the salts present in embryo medium (Section 2.6). All agglomerated significantly with hydrodynamic diameters ranging from ~150–1000× larger than the corresponding primary particle size. The variability in count rates and decreasing size trends observed during DLS acquisition indicated particle sedimentation in embryo medium making size and charge accuracy questionable besides knowing that the particles were very large. Therefore, we not only exposed zebrafish embryos to MO NPs and bulk control material prepared in embryo medium but also MO NPs and bulk controls prepared in ultrapure water to reduce agglomeration, enhance dispersion and maximize bioavailability [43] for the toxicity assessments. MO NPs suspension in ultrapure water reduced the average hydrodynamic diameter, but the particles remained large (>~350 nm diameter). However, TiO_2 NP (TC009), CeO_2 NP (QK055) and ZnO NP were stable enough in ultrapure water suspension to provide precise DLS data (Table 1) These three MO NPs were of similar hydrodynamic size (~353–416 nm) and all three possessed similar, high positive charges especially TiO_2 NP (TC009) and ZnO NP at ~17.1 and 20.2 mV respectively (Table 1, Fig. 1). While CeO_2 NP (QK020) possessed a significantly smaller mean diameter when prepared in water, charge measurements near neutrality (−3.54 mV) indicated instability of the suspension.

3.2. Only zinc oxide nanoparticles demonstrate acute embryonic zebrafish toxicity

Our embryonic zebrafish toxicity assay involves assessing not only lethality from the seven MO NP and bulk control exposures, but also phenotypic malformations that accompany the disruption of key developmental processes that occur during the 8–120 hpf exposure period. We visually inspected exposed 24 hpf embryos for mortality, alterations in spontaneous tail flexion, notochord malformations as well as delayed developmental progression. At 120 hpf, we evaluated all exposed zebrafish larvae for the presence or absence of mortality, 14 morphological

Table 1
Metal oxide nanoparticle physical characterization.

Nanoparticle material	Primary size ± SE (nm)	Hydrodynamic diameter ± SE (nm)	Charge ± SE (mV)	Poly dispersity index ± SE	Mob ± SE (μm cm/V s)
		In embryo medium			
TiO_2 (TC009)	11.64 ± 0.26	2110 ± 73.2	−15.1 ± 0.370	0.483 ± 0.0327	−1.18 ± 0.0290
TiO_2 (TC010)	10.47 ± 0.13	2550 ± 102	−19.2 ± 0.323	0.479 ± 0.0176	−1.50 ± 0.0256
CeO_2 (QK020)	2.87 ± 0.12	2960 ± 112	−8.74 ± 0.561	0.512 ± 0.0242	−0.686 ± 0.0440
CeO_2 (QK055)	2.77 ± 0.12	2150 ± 107	−3.27 ± 0.207	0.584 ± 0.0139	0.256 ± 0.0161
ZnO (BI010)	8.35	1280 ± 79.7	−18.5 ± 0.260	0.366 ± 0.0343	−1.45 ± 0.0199
SnO_2 (UG022)	2.99 ± 0.08	1470 ± 149	−12.2 ± 0.852	0.470 ± 0.0372	−0.957 ± 0.665
SnO_2 (UG023)	2.87 ± 0.06	2120 ± 129	−13.6 ± 0.232	0.549 ± 0.0531	−1.06 ± 0.0190
		In ultrapure water			
TiO_2 (TC009)		416 ± 15.0	17.1 ± 1.47	0.445 ± 0.0238	1.34 ± 0.115
TiO_2 (TC010)		2170 ± 119	−10.6 ± 5.69	0.542 ± 0.0444	−0.830 ± 0.446
CeO_2 (QK020)		521 ± 24.7	−3.54 ± 0.921	0.514 ± 0.004	−0.277 ± 0.0721
CeO_2 (QK055)		353 ± 23.6	38.8 ± 2.76	0.432 ± 0.0345	3.04 ± 0.216
ZnO (BI010)		400 ± 3.72	20.2 ± 0.748	0.151 ± 0.010	1.59 ± 0.0586
SnO_2 (UG022)		1690 ± 151	−8.49 ± 4.08	0.571 ± 0.0349	−0.667 ± 0.320
SnO_2 (UG023)		1210 ± 102	−14.2 ± 3.81	0.553 ± 0.0244	−1.11 ± 0.299

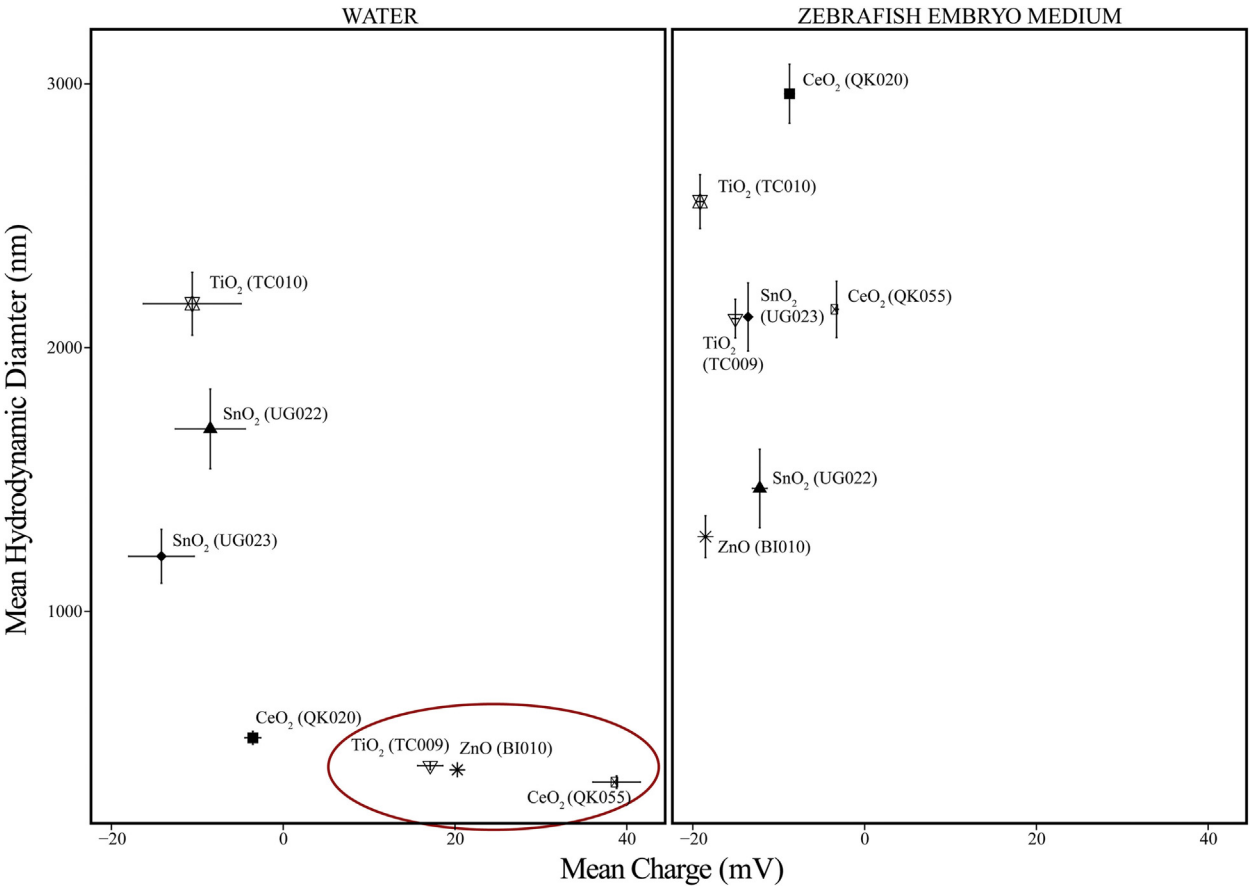

Fig. 1. Dynamic light scattering measurements of 50 mg/L metal oxide nanoparticles (MO NPs) suspended in ion-free medium (water) and high ionic strength medium (zebrafish embryo medium). Error bars represent standard error of the mean ($n = 4$) of hydrodynamic diameter vertically and charge horizontally. Red circle highlights the MO NPs with very similar sizes and charges that created stable suspensions when prepared in water, however, only ZnO was the only MO NP to cause significant mortality and malformations in the five-day embryonic zebrafish bioassay with water as the exposure medium.

endpoints, and one behavioral endpoint (Table 2). Some of the morphological endpoints assessed include axial, craniofacial, somite, fin defects and edema indicating disruption of key processes during organogenesis or in the case of edema, aberrant ion regulation.

Inspection of toxicity data from MO NPs prepared in water or embryo medium compared to respective bulk controls demonstrated most had little to no significant concentration-dependent toxicity, NP or media- specific effects (Fig. A2). For ease of analysis, we condensed the toxicity data into 24 hpf mortality, total mortality, and cumulatively affected zebrafish, which consisted of any 120 hpf malformation and mortality. Agglomeration certainly limited bioavailability of some of the MO NPs contributing, at least in part, to the low observed toxicity especially in the exposures with embryo medium. Yet some MO NP agglomerates, mainly ZnO and TiO_2, have been demonstrated to cause toxicity in adult and embryonic zebrafish under similar waterborne assay conditions as our experiments [34,36,38,50]. Exact logistic regression of the condensed MO NP data revealed that ZnO NP prepared in water produced statistically significant concentration-dependent toxicity after five days of exposure (Fig. 2). Across three experiments, the point estimate of the LC50 ranged between 3.5 and 9.1 mg/L while the EC50, represented by mortality combined with malformed, ranged from 0.5 to 3.51 mg/L. These results coincide well with Zhu et al. who found, in a slightly shorter zebrafish embryo-larval assay, that ZnO NPs prepared in water had an LC50 of 1.793 mg/L. Unlike Zhu et al., our ZnO bulk control caused no significant toxicity when prepared in ultrapure water or embryo medium (Fig. 2). Two independent studies evaluating the toxicity of ZnO NPs to microalgae also found no significant difference between the LC50 of ZnO NP and bulk [51,52]. The magnitude and similarity in dissolution of ZnO NP and bulk led authors from both studies to conclude toxicity was attributed primarily to dissolved zinc ions. The discrepancy in our data may be due to the inherently greater total surface area of ZnO NPs compared to bulk, which could result in a higher degree of dissolution [53,54].

While ZnO NPs were the only material to cause toxicity in our assay, this toxicity appeared to be independent of hydrodynamic size or charge. Both TiO_2 (TC009) and CeO_2 (QK055) exhibited similar mean hydrodynamic sizes and positive charges when prepared in ultrapure water (Table 1, Fig. 1), but did not cause a significant toxic response in the embryonic zebrafish assay (Fig. A2). This

Table 2
Descriptions of time points and endpoints assessed during five-day embryonic zebrafish bioassay.

Abbreviation	Endpoint description	Assessed time point (hours post fertilization)
MO24	Mortality	24
DP24	Delayed developmental progression	24
SM24	Reduced or excessive frequency of zebrafish spontaneous tail coiling	24
NC24	Notochord malformations	24
MORT	Total mortality	120
YSE_	Yolk sac edema	120
AXIS	Abnormal body axis curvature such as lordosis or scoliosis of the spine	120
EYE_	Eye malformations such as large or small eyes	120
SNOU	Snout malformations	120
JAW_	Jaw malformations	120
OTIC	Otic vesicle malformations	120
PE__	Pericardial edema	120
BRAI	Brain malformations such as edema	120
SOMI	Abnormal somite development	120
PFIN	Pectoral fin malformations	120
PIG_	Abnormal pigmentation (hypo or hyper pigmentation)	120
CIRC	Abnormal circulation or vasculature	120
TRUN	Truncated body	120
SWIM	Abnormal swim bladder development	120
NC__	Notochord malformations	120
AFTD	Total mortality combined with any malformation at 120	120

result is contrary to some research, which suggests that positively charged nanoparticles are more likely to induce toxicity than negative or neutrally charged nanoparticles of similar size [2,28], which was not the case in our assay. However, these studies were conducted with different core materials and their nanoparticles were covalently functionalized to create charge [2,28] whereas our MO NPs lacked coating and surface functionalization. The low toxicity associated with zebrafish exposure to TiO_2 NP and TiO_2 agglomerates in the absence of photoactivation during development corroborates other research. For instance, Zhu et al. reported that exposures of up to 10× our highest exposure concentration (500 mg/L) TiO_2 NPs with mean diameters ~ half the size of ours had no significant influence on zebrafish hatch or mortality. No data on TiO_2 NP charge in suspension was provided [55]. Griffitt et al. also reported little to no lethality associated with 48 h exposure to both adult and zebrafish fry (<24 h old) using slightly larger TiO_2 NPs (687.5 nm) than ours with a highly negative charge (−25.1 mV) [56]. The low toxicity of CeO_2 particles in our assay falls in line with other research which, in some cases, considers CeO_2 NPs as inert, biocompatible [57,58] or perhaps beneficial with cytoprotective effects [18]. However, others have reported some acute mortality to the aquatic invertebrate *Daphnia magn*a (LC50 = 12 mg/L) [24]. Differences in CeO_2 NP size (6.7 nm diameter), coating with hexamethylenetetramine or species sensitivity may explain these results. The low biological response associated with both TiO_2 and CeO_2 exposure suggests perhaps charge has little influence on embryonic zebrafish acute toxicity when the particles are in the size range tested in these studies especially without photoactivation of TiO_2. Calculation of the specific surface area of ZnO, TiO_2 (TC009) and CeO_2 (QK055) NPs using the mean hydrodynamic radius revealed only small differences at 267,000, 341,000 and 222,000 cm^2/g respectively. Charge, size and specific surface area were not good predictors of toxicity in our study. Our results suggest a material specific driver of toxicity amongst our ZnO, TiO_2 (TC009) and CeO_2 (QK055) NPs, which may be explained by the propensity of ZnO to dissolve.

3.3. Zinc oxide nanoparticle dissolution analysis and toxicity

Several studies attributed the toxicity of ZnO NPs in waterborne assays to dissolved zinc ions [32,41,51,52,59–62], therefore, we wanted to determine the degree of zinc dissolution from our ZnO NPs to differentiate particle toxicity from ion toxicity in our assay. We utilized ultrafiltration and ICP-OES to separate and quantify what we defined as the soluble zinc fraction (zinc that filtered through a 10 kD membrane) compared to the total concentration of ZnO NP and bulk (Fig. 3). We measured dissolution of two concentrations of ZnO NP: one low (0.625 mg/L) and one high (10 mg/L) and found that there was a high initial level of soluble zinc present in both nanoparticle samples compared to the total zinc, ~47 and 44% respectively. The percent of soluble zinc remained relatively stable over 24 h but increased to ~87% after 120 h in the 10 mg/L (nominal) ZnO NP sample. The 10 mg/L (nominal) ZnO bulk sample generally had a lower percentage of soluble zinc relative to the total, over all tested time points (Fig. 3). As with ZnO NP, the percentage of soluble zinc in the bulk sample increased over time from 26% initially to 66% after 120 h. We predicted the larger ZnO bulk particles to have lower levels of soluble zinc compared to nanoparticles due to reduced total surface compared to the nanoparticles [43,53,54]. Our nominal concentration of zinc differed from the total measured by ICP-OES (Fig. 3). Our 0.625 and 10 mg/L ZnO NP samples should have contained ~0.5 and 8 mg/L zinc, yet we actually measured ~0.2–0.3 and ~4–5 mg/L total zinc respectively. The actual total zinc in the 10 mg/L bulk sample was also different from the nominal at ~0.93–0.98 mg/L. We adjusted the exposure concentrations based on the difference between actual and nominal zinc and compared the toxicity between ZnO bulk and nanoparticles at equivalent concentrations and found the nanoparticles were still more toxic than the bulk. For instance, the actual concentration of ZnO in the nominal 50 mg/L ZnO bulk exposure was ~6 mg/L. The nominal 10 mg/L ZnO NP exposure was actually ~5 mg/L. By comparing the toxicity results of these two adjusted exposure concentrations, we found that ~5 mg/L ZnO NP still caused at least 50% mortality while the bulk caused

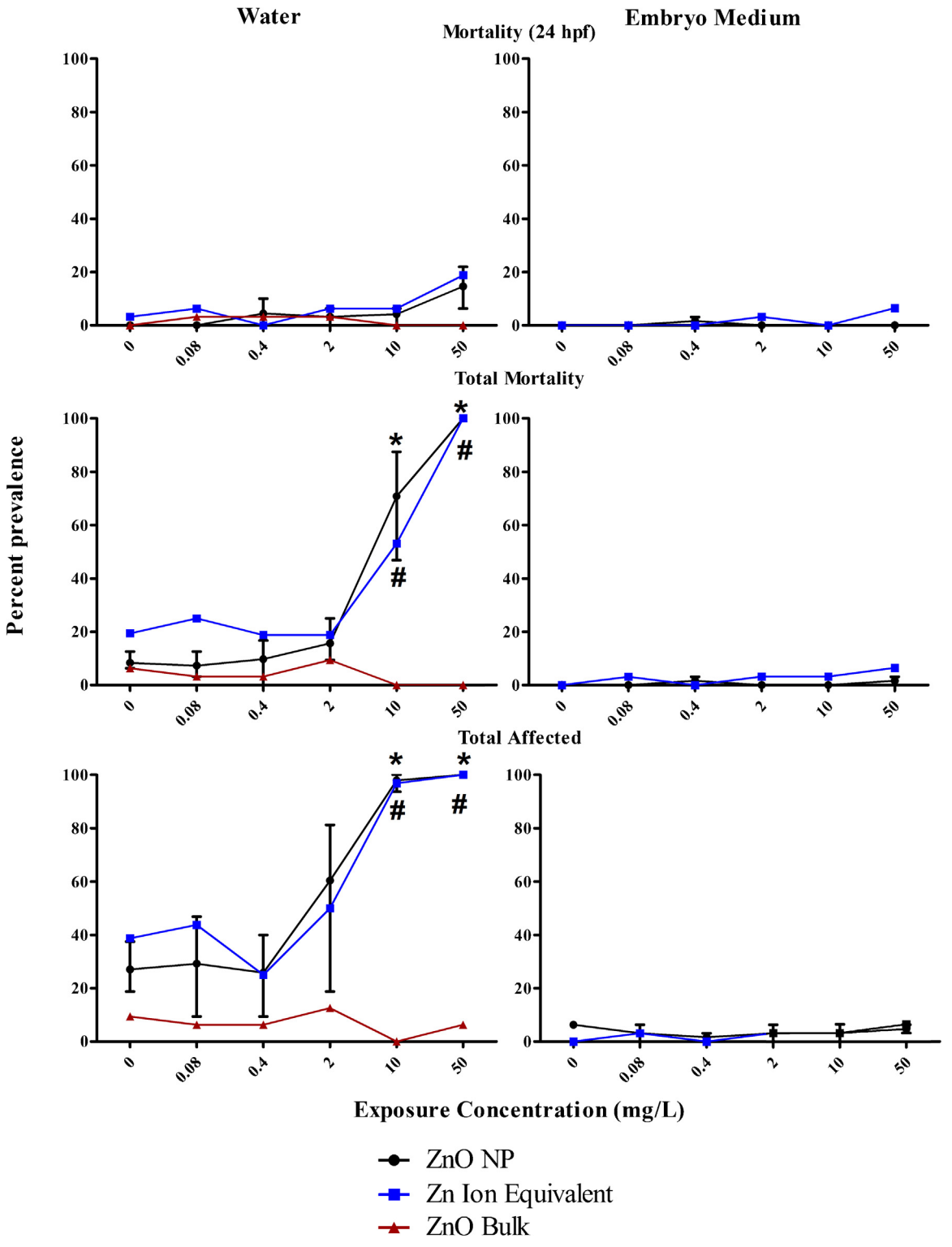

Fig. 2. Toxicity of zinc oxide nanoparticles (ZnO NP) compared to ZnO bulk and Zn ion equivalent controls with 0.5% DMSO vehicle in five-day embryonic zebrafish bioassay under two medium conditions (water and embryo medium). The Zn ion equivalent represents the approximate amount of dissolved zinc present in ZnO NP samples as determined by inductively coupled plasma optical emission spectrometry. Total affected represents the combined percent of zebrafish with mortality or any morphological malformation(s) at 120 h post fertilization. For the ZnO NP prepared in water and embryo medium, the error bars represent the range in mean percent response (3 experiments and 2 experiments respectively, $n = 32$ per experiment per concentration). For the other exposures, the data represents the percent response of 1 experiment, $n = 32$ per concentration. For ZnO NP (*) and Zn ion equivalent ($^{\#}$) data, symbol indicates concentrations where percent prevalence is significantly above background ($p < 0.05$ Fisher's Exact Test) for all experiments studied.

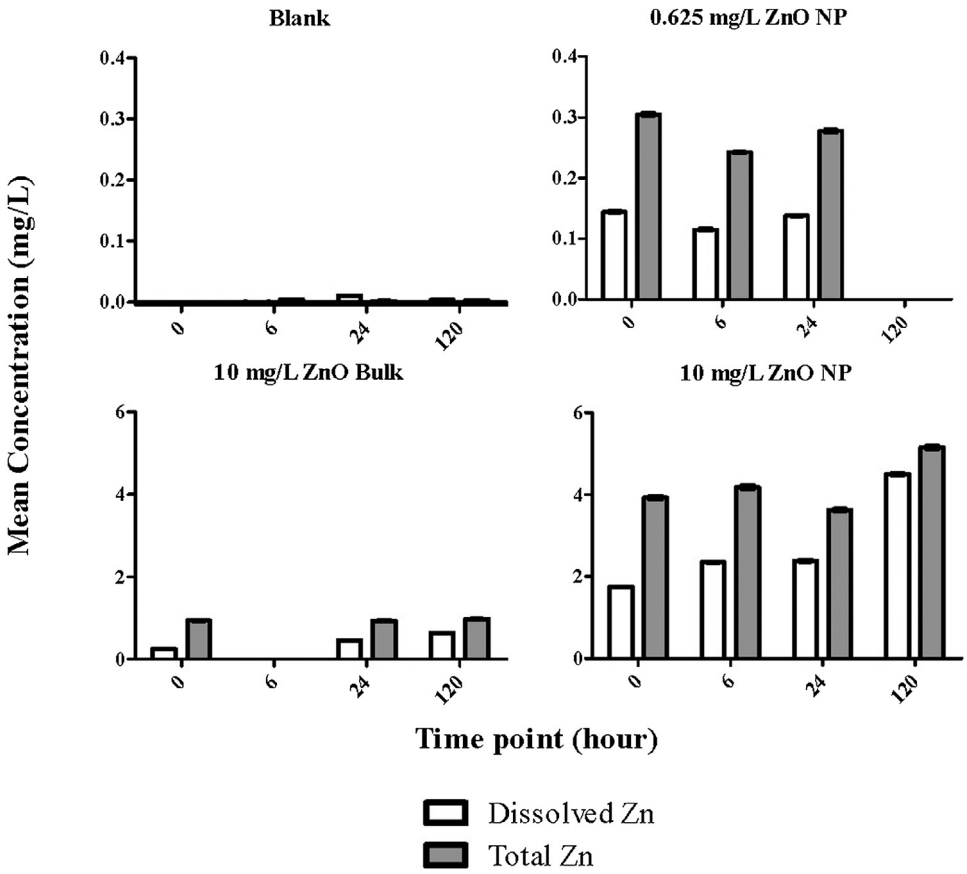

Fig. 3. Dissolved zinc (Zn) present in blanks (0.5% DMSO in ultrapure water), 0.625 and 10 mg/L zinc oxide nanoparticle (ZnO NP) and 10 mg/L ZnO Bulk suspensions prepared in 0.5% DMSO, ultrapure water as measured by ICP-OES over different time points. Error bars represent ±SD, $n = 3$.

0% mortality at a slightly higher exposure concentration (Fig. 2). Therefore, we could conclude that the ZnO NP was more toxic than the ZnO bulk under these assay conditions.

Using the 4.5 mg/L of soluble zinc measured at 120 h as a maximum amount of dissolved zinc present in 10 mg/L ZnO NP sample, we conducted the five-day embryonic zebrafish assay to understand whether exposure to zinc ion could result in similar toxicity as ZnO NP. We exposed 8 hpf embryos to a five-fold concentration series of Zn ion equivalent (98.9–0.16 mg/L $ZnSO_4{\cdot}7H_2O$) prepared in ultrapure water. The mortality and total affected zebrafish results were similar between ZnO NP and the ion equivalent across all tested concentrations. This suggested that the zinc ions could be the main driver of ZnO NP toxicity in water for our assay (Fig. 2). Our results corroborate several other studies. In a freshwater microalgae exposure, Franklin et al., demonstrated that ZnO bulk, ZnO NP and $ZnCl_2$ all had similar IC50 values at ~60 μg Zn/L, which they attributed to the dissolved (0.1 μm filterable) zinc present the in samples [51]. Heinlaan et al. found that both ZnO NP and $ZnSO_4{\cdot}7H_2O$ had similar EC50 values in their bacterial assay at 1.9 and 1.1 mg/L, respectively [59]. Exposure of embryonic zebrafish by Brun et al. to ZnO NP and equivalent dissolved zinc revealed similar uptake and tissue distribution as measured by laser ablation ICP-MS [32].

3.4. Zinc oxide exposure results in life stage-dependent zebrafish toxicity

Due to the unique advantages of the zebrafish embryo-larval test, we can start exposures at different stages of key developmental processes such as somitogenesis, neurogenesis, hepatogenesis, etc. to understand how the nanoparticle is causing toxicity. Because ZnO and zinc ion caused significant toxicity in the five-day embryonic zebrafish assay, we wanted to determine when toxicity was occurring. We exposed 96 hpf zebrafish larvae to ZnO NP, ZnO bulk and Zn ion equivalent, assuming ~48% of the ZnO NP suspension was dissolved zinc based on ICP-OES results. While most major organs are developed by this life stage, the gills are still undergoing maturation. Surprisingly, exposure to the ZnO NPs starting at 96 hpf resulted in a substantial increase in mortality after 24 h of exposure (LC50 = 2.20 mg/L, Fig. 4) compared to 24 h mortality from exposures starting at 8 hpf (~LC50 at 50+ mg/L, Fig. 2). Exposure to Zn ion equivalents resulted in a similar life-stage dependent toxicity as ZnO NP, whereas ZnO bulk did not cause significant mortality compared to vehicle control (Fig. 4). We also observed the presence of skin ulcerations along the body axis of ZnO NP and zinc ion exposed larvae within 1–2 h, which were not apparent in the vehicle or bulk controls. The skin ulcerations were similar in

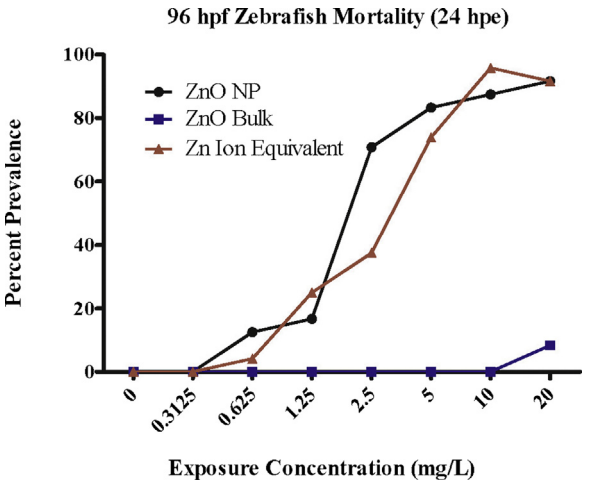

Fig. 4. Larval zebrafish mortality 24 h post exposure (hpe) to zinc oxide nanoparticle (ZnO NP) ($n = 24$ per concentration) ZnO Bulk ($n = 24$ per concentration) and Zn Ion Equivalent ($n = 32$ per concentration) prepared in ultrapure water assuming ~48% nanoparticle dissolution. Exposures started when zebrafish were 96 h post fertilization (hpf).

appearance to those observed by Zhu et al., upon exposure of zebrafish to their ZnO NPs [55]. Scanning electron microscopy images of zebrafish larvae exposed for ~1–2 h prior to fixation revealed that the ZnO NPs caused external damage over the entire body including gill primordia, which was not apparent in the vehicle controls (Fig. A3). Ulcerations appeared to concentrate around neuromasts of the lateral line but it was difficult to discern if this led lethality. George et al., demonstrated that ZnO NPs are capable of disrupting plasma membrane integrity in macrophage and epithelial cell lines [63], which may explain why we observed tissue ulceration. An acridine orange/ethidium bromide assay demonstrated that exposure of isopods to nanoscale ZnO resulted in cell membrane destabilization in the hepatopancreas [64]. Xiong et al. found that 5 mg/L ZnO NP induced gill cell shrinkage in adult zebrafish but not necessarily cell membrane rupture after 96 h of exposure [50]. Perhaps the ZnO NPs and/or zinc ions present in the exposure disrupted the larval zebrafish epidermal cells over the entire body axis including gill primordia, which eventually resulted in mortality. Gills are known to be a primary target of ZnO NPs in oysters [65]. Our results suggest that later zebrafish life stages may be more sensitive than the embryonic stage, which could confound predictive toxicity interpretation. Results by Ma and Diamond support this conclusion [35]. However, they attributed their life-stage dependent differences in toxicity to the presence of the chorion, which impedes nanoparticle bioavailability when exposures start at earlier life stages. This is different from our assay as we enzymatically remove the chorion. Nevertheless, it illustrates that we must carefully consider possible limitations of these exposure paradigms in toxicity assessments.

4. Conclusions

The objective of these studies was to assess and compare the *in vivo* toxicity of seven novel MO NPs made from ZnO, TiO_2, CeO_2 and SnO_2 that were uncoated and without surface functionalization using an embryonic zebrafish assay. We hypothesized the physicochemical properties hydrodynamic size and charge would dictate *in vivo* toxicity. However, little toxicity was observed, partly due to MO NP agglomeration, which reduced bioavailability and made size and charge measurements challenging. Three MO NPs created stable suspension in low ionic strength ultrapure water: TiO_2 (TC009), CeO_2 (QK055) and ZnO. While all three MO NPs possessed similar mean hydrodynamic diameters and charges, only ZnO was significantly toxic with a point estimate LC50 ranging between 3.5 and 9.1 mg/L.

Further investigation into ZnO toxicity revealed that it was life stage dependent. The 24 h toxicity increased greatly (~22.7 fold) when zebrafish exposures started at the larval life stage (96 hpf) compared to the 24 h toxicity following embryonic exposure (8 hpf). This finding is especially important as many laboratories have adopted the five-day embryo-larval zebrafish assay to evaluate and predict *in vivo* toxicity, yet we found that testing at earlier life stages may not be the most sensitive. This sensitivity did not depend on the chorion as we enzymatically remove it for unimpeded exposure. Therefore, it may be necessary to test some materials like ZnO at several early time points to identify the most sensitive window for predicting toxicity for health and safety assessment. Fortunately, we can efficiently examine the factors contributing to adverse biological interactions while working with material scientists to quickly revise synthesis methods to modify material properties followed by re-evaluation of biocompatibility [26]. This approach of using rapid *in vivo* readouts to inform the engineering of safer nanomaterials that maintain their desirable properties is consistent with the principles of green chemistry and green nanoscience [66].

Because ZnO NP toxicity is frequently associated with dissolution [32,41,51,52,59–62], we quantified the amount released zinc ion (10 kD filterable). We found high levels of zinc ion (40–89% of total sample) were generated in our ZnO NP suspensions. Exposure of zebrafish to zinc ion equivalents suggested dissolved zinc ion may be a major contributor to ZnO toxicity at both embryonic and larval zebrafish life stages when exposures occurred in ultrapure water. Therefore, we conclude that elemental composition and dissolution potential were key drivers of toxicity amongst ZnO, TiO_2 (TC009) and CeO_2 (QK055) rather than hydrodynamic size and charge in water suspensions.

Another important discovery of these experiments was that a careful understanding of how assay conditions, such as medium ion composition and strength, are important in interpreting MO NP results. Conducting our assay using high ionic strength embryo medium reduced bioavailability through agglomeration of the MO NPs, thereby reducing zebrafish toxicity. This is not necessarily a unique conclusion as others have seen similar effects testing silver nanoparticles [45], however, if we had not conducted our assays using ultrapure water as a medium, we may have erroneously concluded that all our MO NPs including ZnO NP were non-toxic to zebrafish and not been able to deduce any relationships between toxicity and physicochemical properties. Caution must be employed in interpretation of data from these waterborne assays especially regarding

potential MO NP agglomeration, sedimentation and/or dissolution.

Author contributions

The manuscript was primarily written by Leah C. Wehmas with contributions from Dr. Robert Tanguay, Dr. Alex Punnoose, Dr. Juliet Greenwood and Dr. Cliff Pereira. Catherine Anders and Jordan Chess in Dr. Alex Punnoose's laboratory synthesized all nanomaterials and performed initial characterization (XRD and TEM) of the primary particles. Leah Wehmas conducted DLS, SEM, ICP-OES and all zebrafish toxicity assessments. Dr. Cliff Pereira performed statistical analyses of the data.

Conflicts of interest

The authors declare no conflict of interest.

Transparency document

The Transparency document associated with this article can be found in the online version.

Acknowledgments

We would like to thank Teresa Sawyer and the Oregon State University Electron Microscopy Facility for SEM images and Andy Ungerer of the WM Keck Collaboratory for Plasma Spectrometry at Oregon State University for assistance with ICP-OES. We would also like to thank Dr. Yasmeen Nkrumah-Elie for advice on ICP-OES sample preparation and Dr. Stacey Harper for the use of the Malvern Zetasizer Nano ZS. This research was funded by the NIH T32 ES07060, NIH P30 ES000210 and NSF 1134468.

Appendices.

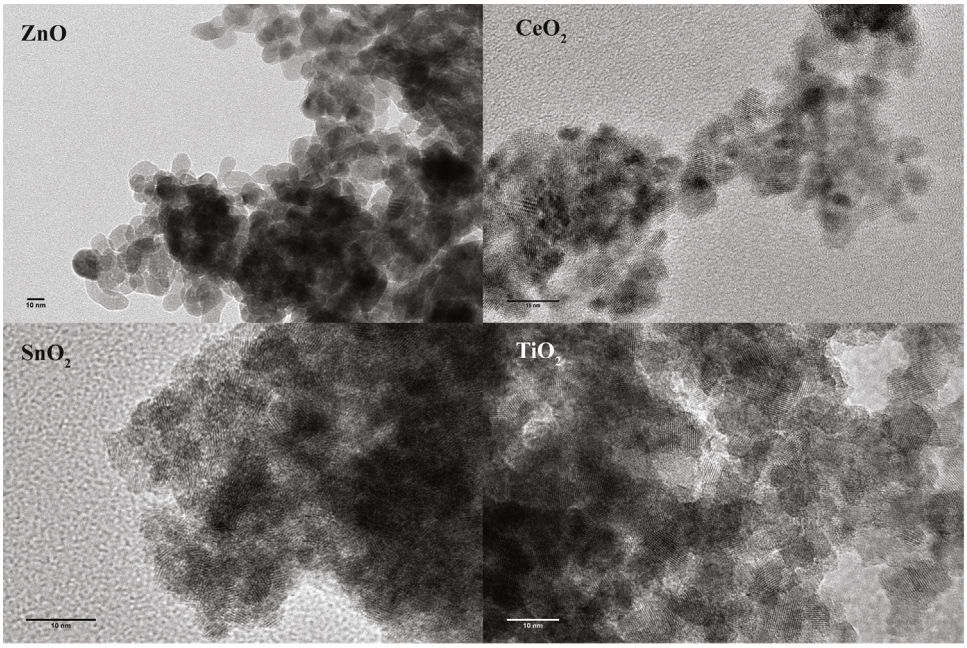

Fig. A1. Representative TEM images of each metal oxide nanoparticle synthesis method. Abbreviations: ZnO = zinc oxide, CeO_2 = cerium dioxide, SnO_2 = tin dioxide, TiO_2 = titanium dioxide.

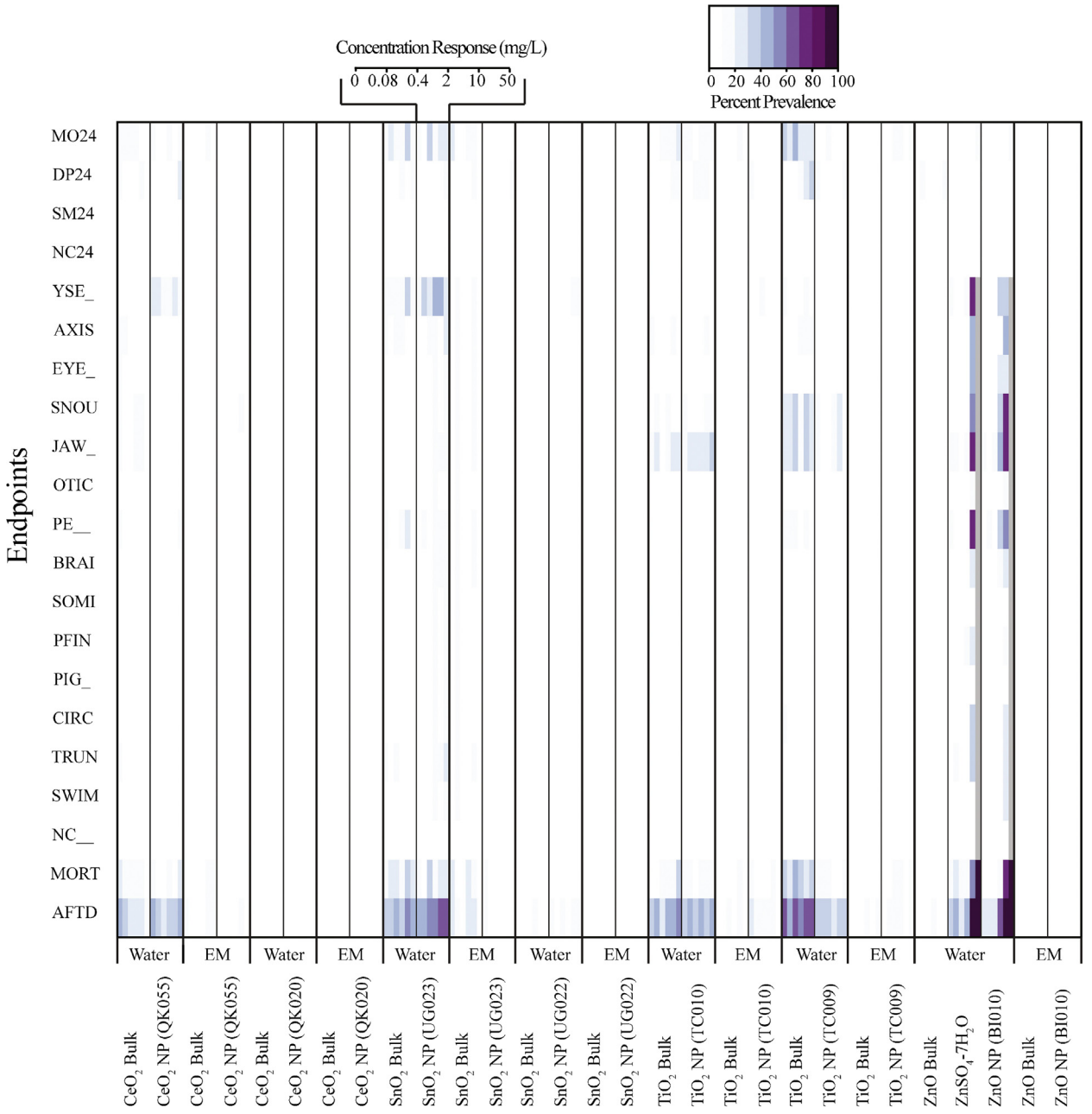

Fig. A2. Heat map displaying the percent prevalence of malformations and mortality resulting from a five-day embryonic zebrafish exposure to a five-fold concentration response series ranging from 0 50 mg/L metal oxide nanoparticles, bulk controls, and, in the case of zinc, a dissolved zinc equivalent (0–99 mg/L) ionic control ($n = 32$ except ZnO NP in water where $n = 96$). Exposures were conducted in ultrapure water or embryo medium (EM). The color scale above the heat map indicates the percent prevalence of a particular endpoint assessed in the zebrafish at 24 h post fertilization (hpf) or 120 hpf. Abbreviations for endpoints assessed at 24 hpf: MO24 = mortality, DP = delayed developmental progression, SM = reduced or excessive frequency of zebrafish spontaneous tail coiling, and NC24 = notochord malformation. Abbreviations for endpoints assessed at 120 hpf: YSE = yolk sac edema, AXIS = abnormal body axis curvature, EYE = eye malformation, SNOU = snout malformation, JAW = jaw malformation, OTIC = otic vesicle malformation, PE = pericardial edema, BRAIN = brain malformation, SOMI = abnormal somite development, PFIN = malformed pectoral fins, PIG = hypo or hyper pigmentation, CIRC = abnormal circulation or circulatory vasculature, TRUN = shorted body axis, SWIM = abnormal swim bladder development, NC = notochord malformation, MORT = total mortality, and AFTD = total dead and malformed larvae.

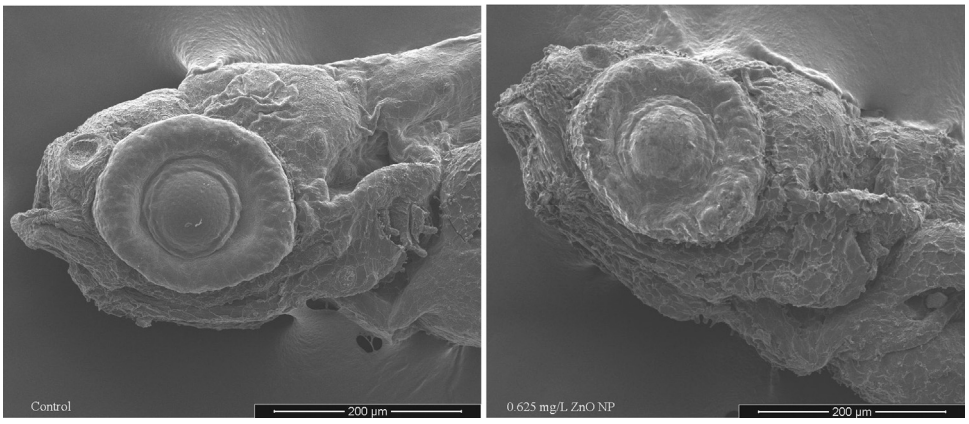

Fig. A3. Representative scanning electron microscopy images of 96 hpf zebrafish exposed to zinc oxide nanoparticle (ZnO NP) and control prepared in ultrapure water for ~1–2 h prior to fixation.

References

[1] A. Nel, T. Xia, L. Mädler, N. Li, Toxic potential of materials at the nanolevel, Science 311 (2006) 622–627.
[2] G. Oberdörster, E. Oberdörster, J. Oberdörster, Nanotoxicology: an emerging discipline evolving from studies of ultrafine particles, Environ. Health Perspect. 113 (2005) 823.
[3] L.K. Adams, D.Y. Lyon, P.J.J. Alvarez, Comparative eco-toxicity of nanoscale TiO_2, SiO_2, and ZnO water suspensions, Water Res. 40 (2006) 3527–3532.
[4] Q. Li, S. Mahendra, D.Y. Lyon, L. Brunet, M.V. Liga, D. Li, P.J. Alvarez, Antimicrobial nanomaterials for water disinfection and microbial control: potential applications and implications, Water Res. 42 (2008) 4591–4602.
[5] M. Premanathan, K. Karthikeyan, K. Jeyasubramanian, G. Manivannan, Selective toxicity of ZnO nanoparticles toward gram-positive bacteria and cancer cells by apoptosis through lipid peroxidation, Nanomed. Nanotechnol. Biol. Med. 7 (2011) 184–192.
[6] K.M. Reddy, K. Feris, J. Bell, D.G. Wingett, C. Hanley, A. Punnoose, Selective toxicity of zinc oxide nanoparticles to prokaryotic and eukaryotic systems, Appl. Phys. Lett. 90 (2007) 213902.
[7] H. Lee, M.K. Yu, S. Park, S. Moon, J.J. Min, Y.Y. Jeong, H.W. Kang, S. Jon, Thermally cross-linked superparamagnetic iron oxide nanoparticles: synthesis and application as a dual imaging probe for cancer in vivo, J. Am. Chem. Soc. 129 (2007) 12739–12745.
[8] J.H. Lee, Y.M. Huh, Y.W. Jun, J.W. Seo, J.T. Jang, H.T. Song, S. Kim, E.J. Cho, H.G. Yoon, J.S. Suh, et al., Artificially engineered magnetic nanoparticles for ultra-sensitive molecular imaging, Nat. Med. 13 (2007) 95–99.
[9] M. Liong, J. Lu, M. Kovochich, T. Xia, S.G. Ruehm, A.E. Nel, F. Tamanoi, J.I. Zink, Multifunctional inorganic nanoparticles for imaging, targeting, and drug delivery, ACS Nano 2 (2008) 889–896.
[10] H. Wang, D. Wingett, M.H. Engelhard, K. Feris, K.M. Reddy, P. Turner, J. Layne, C. Hanley, J. Bell, D. Tenne, et al., Fluorescent dye encapsulated ZnO particles with cell-specific toxicity for potential use in biomedical applications, J. Mater. Sci. Mater. Med. 20 (2008) 11–22.
[11] M.K. Yu, J. Park, Y.Y. Jeong, W.K. Moon, S. Jon, Integrin-targeting thermally cross-linked superparamagnetic iron oxide nanoparticles for combined cancer imaging and drug delivery, Nanotechnology 21 (2010) 415102.
[12] K.H. Bae, K. Lee, C. Kim, T.G. Park, Surface functionalized hollow manganese oxide nanoparticles for cancer targeted sirna delivery and magnetic resonance imaging, Biomaterials 32 (2011) 176–184.
[13] H. Hong, J. Shi, Y. Yang, Y. Zhang, J.W. Engle, R.J. Nickles, X. Wang, W. Cai, Cancer-targeted optical imaging with fluorescent zinc oxide nanowires, Nano Lett. 11 (2011) 3744–3750.
[14] C. Hanley, J. Layne, A. Punnoose, K.M. Reddy, I. Coombs, A. Coombs, K. Feris, D. Wingett, Preferential killing of cancer cells and activated human t cells using ZnO nanoparticles, Nanotechnology 19 (2008) 295103.
[15] S. Ostrovsky, G. Kazimirsky, A. Gedanken, C. Brodie, Selective cytotoxic effect of zno nanoparticles on glioma cells, Nano Res. 2 (2009) 882–890.
[16] P. Thevenot, J. Cho, D. Wavhal, R.B. Timmons, L. Tang, Surface chemistry influences cancer killing effect of TiO_2 nanoparticles, Nanomed. Nanotechnol. Biol. Med. 4 (2008) 226–236.
[17] V. Sharma, R.K. Shukla, N. Saxena, D. Parmar, M. Das, A. Dhawan, DNA damaging potential of zinc oxide nanoparticles in human epidermal cells, Toxicol. Lett. 185 (2009) 211–218.
[18] T. Xia, M. Kovochich, M. Liong, L. Madler, B. Gilbert, H. Shi, J.I. Yeh, J.I. Zink, A.E. Nel, Comparison of the mechanism of toxicity of zinc oxide and cerium oxide nanoparticles based on dissolution and oxidative stress properties, ACS Nano 2 (2008) 2121–2134.
[19] Q. Rahman, M. Lohani, E. Dopp, H. Pemsel, L. Jonas, D.G. Weiss, D. Schiffmann, Evidence that ultrafine titanium dioxide induces micronuclei and apoptosis in syrian hamster embryo fibroblasts, Environ. Health Perspect. 110 (2002) 797.
[20] J.-R. Gurr, A.S.S. Wang, C.-H. Chen, K.-Y. Jan, Ultrafine titanium dioxide particles in the absence of photoactivation can induce oxidative damage to human bronchial epithelial cells, Toxicology 213 (2005) 66–73.
[21] C.M. Sayes, R. Wahi, P.A. Kurian, Y. Liu, J.L. West, K.D. Ausman, D.B. Warheit, V.L. Colvin, Correlating nanoscale titania structure with toxicity: a cytotoxicity and inflammatory response study with human dermal fibroblasts and human lung epithelial cells, Toxicol. Sci. 92 (2006) 174–185.
[22] T.J. Brunner, P. Wick, P. Manser, P. Spohn, R.N. Grass, L.K. Limbach, A. Bruinink, W.J. Stark, In vitro cytotoxicity of oxide nanoparticles: comparison to asbestos, silica, and the effect of particle solubility†, Environ. Sci. Technol. 40 (2006) 4374–4381.
[23] W. Lin, Y.W. Huang, X.D. Zhou, Y. Ma, Toxicity of cerium oxide nanoparticles in human lung cancer cells, Int. J. Toxicol. 25 (2006) 451–457.
[24] A. García, R. Espinosa, L. Delgado, E. Casals, E. González, V. Puntes, C. Barata, X. Font, A. Sánchez, Acute toxicity of cerium oxide, titanium oxide and iron oxide nanoparticles using standardized tests, Desalination 269 (2011) 136–141.
[25] V.E. Fako, D.Y. Furgeson, Zebrafish as a correlative and predictive model for assessing biomaterial nanotoxicity, Adv. Drug Deliv. Rev. 61 (2009) 478–486.
[26] S.L. Harper, J.A. Dahl, B.L.S. Maddux, R.L. Tanguay, J.E. Hutchison, Proactively designing nanomaterials to enhance performance and minimise hazard, Int. J. Nanotechnol. 5 (2008) 124–142.
[27] C.Y. Usenko, S.L. Harper, R.L. Tanguay, In vivo evaluation of carbon fullerene toxicity using embryonic zebrafish, Carbon 45 (2007) 1891–1898.
[28] S.L. Harper, J.L. Carriere, J.M. Miller, J.E. Hutchison, B.L.S. Maddux, R.L. Tanguay, Systematic evaluation of nanomaterial toxicity: utility of standardized materials and rapid assays, ACS Nano 5 (2011) 4688–4697.
[29] L. Truong, S.L. Harper, R.L. Tanguay, Evaluation of embryotoxicity using the zebrafish model, Methods Mol. Biol. 691 (2011) 271–279.
[30] W. Bai, Z. Zhang, W. Tian, X. He, Y. Ma, Y. Zhao, Z. Chai, Toxicity of zinc oxide nanoparticles to zebrafish embryo: a physicochemical study of toxicity mechanism, J. Nanopart. Res. 12 (2010) 1645–1654.
[31] O. Bar-Ilan, K.M. Louis, S.P. Yang, J.A. Pedersen, R.J. Hamers, R.E. Peterson, W. Heideman, Titanium dioxide nanoparticles produce

phototoxicity in the developing zebrafish, Nanotoxicology 6 (2012) 670–679.
[32] N.R. Brun, M. Lenz, B. Wehrli, K. Fent, Comparative effects of zinc oxide nanoparticles and dissolved zinc on zebrafish embryos and eleuthero-embryos: importance of zinc ions, Sci. Total Environ. 476-477 (2014) 657–666.
[33] T.-H. Chen, C.-Y. Lin, M.-C. Tseng, Behavioral effects of titanium dioxide nanoparticles on larval zebrafish (*danio rerio*), Mar. Pollut. Bull. 63 (2011) 303–308.
[34] M. Faria, J.M. Navas, A.M.V.M. Soares, C. Barata, Oxidative stress effects of titanium dioxide nanoparticle aggregates in zebrafish embryos, Sci. Total Environ. 470-471 (2014) 379–389.
[35] H. Ma, S.A. Diamond, Phototoxicity of TiO_2 nanoparticles to zebrafish (*danio rerio*) is dependent on life stage, Environ. Toxicol. Chem. 32 (2013) 2139–2143.
[36] L.-p. Yu, T. Fang, D.-w. Xiong, W.-t. Zhu, X.-f. Sima, Comparative toxicity of nano-ZnO and bulk ZnO suspensions to zebrafish and the effects of sedimentation, [radical dot]OH production and particle dissolution in distilled water, J. Environ. Monit. 13 (2011) 1975–1982.
[37] X. Zhao, S. Wang, Y. Wu, H. You, L. Lv, Acute Zno nanoparticles exposure induces developmental toxicity, oxidative stress and DNA damage in embryo-larval zebrafish, Aquat. Toxicol. 136-137 (2013) 49–59.
[38] X. Zhu, J. Wang, X. Zhang, Y. Chang, Y. Chen, The impact of zno nanoparticle aggregates on the embryonic development of zebrafish (*danio rerio*), Nanotechnology 20 (2009) 195103.
[39] K.J. Lee, P.D. Nallathamby, L.M. Browning, C.J. Osgood, X.H.N. Xu, In vivo imaging of transport and biocompatibility of single silver nanoparticles in early development of zebrafish embryos, ACS Nano 1 (2007) 133–143.
[40] R.D. Handy, T.B. Henry, T.M. Scown, B.D. Johnston, R.T. Charles, Manufactured nanoparticle: their uptake and effects on fish-a mechanistic analysis, Ecotoxicology 17 (2008) 396–409.
[41] I. Blinova, A. Ivask, M. Heinlaan, M. Mortimer, A. Kahru, Ecotoxicity of nanoparticles of CuO and ZnO in natural water, Environ. Pollut. 158 (2010) 41–47.
[42] A.A. Keller, H. Wang, D. Zhou, H.S. Lenihan, G. Cherr, B.J. Cardinale, R. Miller, Z. Ji, Stability and aggregation of metal oxide nanoparticles in natural aqueous matrices, Environ. Sci. Technol. 44 (2010) 1962–1967.
[43] S.-W. Bian, I.A. Mudunkotuwa, T. Rupasinghe, V.H. Grassian, Aggregation and dissolution of 4 nm ZnO nanoparticles in aqueous environments: influence of pH, ionic strength, size, and adsorption of humic acid, Langmuir 27 (2011) 6059–6068.
[44] L. Truong, T. Zaikova, E.K. Richman, J.E. Hutchison, R.L. Tanguay, Media ionic strength impacts embryonic responses to engineered nanoparticle exposure, Nanotoxicology 6 (2012) 691–699.
[45] K.T. Kim, L. Truong, L. Wehmas, R.L. Tanguay, Silver nanoparticle toxicity in the embryonic zebrafish is governed by particle dispersion and ionic environment, Nanotechnology 24 (2013) 115101.
[46] L. Lutterotti, S. Matthies, H. Wenk, Maud: a friendly java program for material analysis using diffraction, IUCr: Newsl. CPD (1999) *21*.
[47] H.C. Poynton, J.M. Lazorchak, C.A. Impellitteri, M.E. Smith, K. Rogers, M. Patra, K.A. Hammer, H.J. Allen, C.D. Vulpe, Differential gene expression in *daphnia magna* suggests distinct modes of action and bioavailability for ZnO nanoparticles and Zn ions, Environ. Sci. Technol. 45 (2010) 762–768.
[48] C.B. Kimmel, W.W. Ballard, S.R. Kimmel, B. Ullmann, T.F. Schilling, Stages of embryonic development of the zebrafish, Dev. Dyn. 203 (1995) 253–310.
[49] D. Mandrell, L. Truong, C. Jephson, M.R. Sarker, A. Moore, C. Lang, M.T. Simonich, R.L. Tanguay, Automated zebrafish chorion removal and single embryo placement: optimizing throughput of zebrafish developmental toxicity screens, J. Lab. Automat. 17 (2012) 66–74.
[50] D. Xiong, T. Fang, L. Yu, X. Sima, W. Zhu, Effects of nano-scale TiO_2, ZnO and their bulk counterparts on zebrafish: acute toxicity, oxidative stress and oxidative damage, Sci. Total Environ. 409 (2011) 1444–1452.
[51] N.M. Franklin, N.J. Rogers, S.C. Apte, G.E. Batley, G.E. Gadd, P.S. Casey, Comparative toxicity of nanoparticulate ZnO, bulk ZnO, and $ZnCl_2$ to a freshwater microalga (*pseudokirchneriella subcapitata*): the importance of particle solubility, Environ. Sci. Technol. 41 (2007) 8484–8490.
[52] V. Aruoja, H.-C. Dubourguier, K. Kasemets, A. Kahru, Toxicity of nanoparticles of CuO, ZnO and TiO_2 to microalgae *pseudokirchneriella subcapitata*, Sci. Total Environ. 407 (2009) 1461–1468.
[53] P. Borm, F.C. Klaessig, T.D. Landry, B. Moudgil, J. Pauluhn, K. Thomas, R. Trottier, S. Wood, Research strategies for safety evaluation of nanomaterials, part v: role of dissolution in biological fate and effects of nanoscale particles, Toxicol. Sci. 90 (2006) 23–32.
[54] Z. Yang, C. Xie, Zn^{2+} release from zinc and zinc oxide particles in simulated uterine solution, Colloids Surf. B: Biointerfaces 47 (2006) 140–145.
[55] X. Zhu, L. Zhu, Z. Duan, R. Qi, Y. Li, Y. Lang, Comparative toxicity of several metal oxide nanoparticle aqueous suspensions to zebrafish (*danio rerio*) early developmental stage, J. Environ. Sci. Health A 43 (2008) 278–284.
[56] R.J. Griffitt, J. Luo, J. Gao, J.C. Bonzongo, D.S. Barber, Effects of particle composition and species on toxicity of metallic nanomaterials in aquatic organisms, Environ. Toxicol. Chem. 27 (2009) 1972–1978.
[57] C. Ispas, D. Andreescu, A. Patel, D.V. Goia, S. Andreescu, K.N. Wallace, Toxicity and developmental defects of different sizes and shape nickel nanoparticles in zebrafish, Environ. Sci. Technol. 43 (2009) 6349–6356.
[58] K. Van Hoecke, J.T. Quik, J. Mankiewicz-Boczek, K.A. De Schamphelaere, A. Elsaesser, P. Van der Meeren, C. Barnes, G. McKerr, C.V. Howard, D. Van de Meent, et al., Fate and effects of CeO_2 nanoparticles in aquatic ecotoxicity tests, Environ. Sci. Technol. 43 (2009) 4537–4546.
[59] M. Heinlaan, A. Ivask, I. Blinova, H.C. Dubourguier, A. Kahru, Toxicity of nanosized and bulk ZnO, CuO and TiO_2 to bacteria *vibrio fischeri* and crustaceans daphnia magna and *thamnocephalus platyurus*, Chemosphere 71 (2008) 1308–1316.
[60] X. Deng, Q. Luan, W. Chen, Y. Wang, M. Wu, H. Zhang, Z. Jiao, Nanosized zinc oxide particles induce neural stem cell apoptosis, Nanotechnology 20 (2009) 115101.
[61] W. Song, J. Zhang, J. Guo, J. Zhang, F. Ding, L. Li, Z. Sun, Role of the dissolved zinc ion and reactive oxygen species in cytotoxicity of ZnO nanoparticles, Toxicol. Lett. 199 (2010) 389–397.
[62] E.A. Fairbairn, A.A. Keller, L. Mädler, D. Zhou, S. Pokhrel, G.N. Cherr, Metal oxide nanomaterials in seawater: linking physicochemical characteristics with biological response in sea urchin development, J. Hazard. Mater. 192 (2011) 1565–1571.
[63] S. George, S. Pokhrel, T. Xia, B. Gilbert, Z. Ji, M. Schowalter, A. Rosenauer, R. Damoiseaux, K.A. Bradley, L. Mädler, Use of a rapid cytotoxicity screening approach to engineer a safer zinc oxide nanoparticle through iron doping, ACS Nano 4 (2009) 15–29.
[64] J. Valant, D. Drobne, K. Sepcic, A. Jemec, K. Kogej, R. Kostanjsek, Hazardous potential of manufactured nanoparticles identified by in vivo assay, J. Hazard. Mater. 171 (2009) 160–165.
[65] R. Trevisan, G. Delapedra, D.F. Mello, M. Arl, É.C. Schmidt, F. Meder, M. Monopoli, E. Cargnin-Ferreira, Z.L. Bouzon, A.S. Fisher, et al., Gills are an initial target of zinc oxide nanoparticles in oysters crassostrea gigas, leading to mitochondrial disruption and oxidative stress, Aquat. Toxicol. 153 (2014) 27–38.
[66] L.C. McKenzie, J.E. Hutchison, Green nanoscience: an integrated approach to greener products, processes, and applications, Chem. Today 22 (2004) 25–28.